RECURSIVE ELIMINATION OF TEMPORAL CONTRASTS BETWEEN TIME-LAPSE ACOUSTIC WAVE FIELDS

MENNO DILLEN*, JACOB FOKKEMA and KEES WAPENAAR

Delft University of Technology, Department of Applied Earth Sciences, Delft, The Netherlands.
** Present address: University of Texas at Dallas, Center for Lithospheric Studies, Richardson, Texas, U.S.A.*

(Received September 1, 2001; revised version accepted November 9, 2001)

ABSTRACT

Dillen, M.W.P., Fokkema, J.T. and Wapenaar, C.P.A., 2002. Recursive elimination of temporal contrasts between time-lapse acoustic wave fields. In: Fokkema, J.T. and Wapenaar, C.P.A. (Eds.), Integrated 4D Seismics. *Journal of Seismic Exploration*, 11: 41-57.

A boundary integral representation of the difference of two time-lapse acoustic wave fields is investigated. Recursive computation of the boundary integral eliminates the action of temporal contrast sources above the boundary at which the integral is evaluated. This method is a basis for pre-stack temporal contrast imaging and inversion schemes, analogous to implementations of the Helmholtz integral in inverse scattering theory.

KEY WORDS: time-lapse acoustics, boundary integral method, difference reflection, Dirichlet-to-Neumann operator, reciprocity, pre-stack, directional wavefield, decomposition.

INTRODUCTION

In time-lapse seismology one aims to infer changes in the subsurface stress, pore fluid pressure and pore fluid saturation, either caused by natural phenomena or by human intervention. Non-repeatability of the time-lapse experiments induces additional changes not related to these in-situ physical processes. Because non-repeatability originates from time-lapse changes in the source and receiver domains, the associated time-shift, in a difference gather, is added to the time-shift induced by the physical process one is interested in. Besides non-repeatability, any change in the medium through which the wave

0963-0651/02/$5.00

field travels, above the region of interest, adds to the total time-shift and amplitude change measured at the receivers. The result is often a difference gather in which difference reflections are visible throughout the entire recording time. Statistical processes, denoted by the generic term cross-equalization (e.g. Rickett and Lumley, 2001), have been used to remove the unwanted time-shifts and amplitude changes in post-stack seismic data. In this paper, we propose a pre-stack method based on the wave equation to remove unwanted time-shifts and amplitude changes in a recursive way. The method employs a boundary integral, evaluated at a certain depth, in terms of the two time-lapse wave fields back-propagated to this depth. The resulting interaction of the back-propagated time-lapse wave fields eliminates the effect of temporal contrasts associated to changes in the medium above the interaction depth, provided these changes can be modelled by the wave equation. Hence, it restores the time-shift as well as the amplitude of a desired difference reflection. In this paper, this effect is shown numerically with several finite difference examples. The vanishing of difference reflections in the boundary integral gather, associated with temporal contrasts above the interaction depth, is also shown analytically. To this end, a wave field decomposition is applied to both time-lapse wave fields in terms of Dirichlet-to-Neumann (D-t-N) operators. Substitution of the wave field decompositions into the boundary integral yields a symplectic matrix operator. A symplectic eigenvalue decomposition of this matrix operator gives a new wave field decomposition in terms of symplectic eigenvalue D-t-N operators. On this new basis, these D-t-N operators, and hence the wave field decomposition operators, are identical for both time-lapse wave fields, which explains the vanishing of difference reflections. The described boundary integral method resembles the application of the Kirchhoff (time-domain) or the Helmholtz (frequency-domain) integral representation of a scattered wave field originating from spatial contrasts below the integration depth. In our application the boundary integral represents a difference wave field which can be shown to originate from temporal contrast sources below the integration depth (Dillen et al., 2000).

BOUNDARY INTEGRAL

We consider two sets of time-lapse acoustic wave fields, denoted by *reference* wave fields and *monitor* wave fields, associated with seismic experiments. We assume that the duration of the reference and monitor seismic experiments is much smaller than the time-lapse interval between the two experiments, such that during either seismic experiment the medium parameters may be approximated by constant functions of time. Reference and monitor wave field quantities, pressure p and particle velocity v_k, density ρ and compressibility κ, and sources q and f_k, are denoted by the superscripts $.^{(1)}$ and $.^{(2)}$, respectively. Consider the Fourier domain (signified by $\hat{}$) acoustic reference and monitor wave field equations,

$$\partial_k \hat{p}^{(1),(2)}(\mathbf{x};\mathbf{x}',\omega) + i\omega\rho^{(1),(2)}(\mathbf{x})\hat{v}_k^{(1),(2)}(\mathbf{x};\mathbf{x}',\omega) = \hat{f}_k^{(1),(2)}(\omega)\delta(\mathbf{x}-\mathbf{x}') \quad , \tag{1}$$

$$\partial_k \hat{v}_k^{(1),(2)}(\mathbf{x};\mathbf{x}',\omega) + i\omega\kappa^{(1),(2)}(\mathbf{x})\hat{p}^{(1),(2)}(\mathbf{x};\mathbf{x}',\omega) = \hat{q}^{(1),(2)}(\omega)\delta(\mathbf{x}-\mathbf{x}') \quad , \tag{2}$$

with $\mathbf{x} = (\mathbf{x}_T, x_3) \in \mathbb{R}^3$, in which $\mathbf{x}_T = (x_1, x_2)$ denotes the transverse coordinate, and x_3 denotes the longitudinal coordinate, oriented in the main wave field direction. The source positions of the respective wave fields are indicated in the argument list. The Fourier transform parameter ω is the radial frequency, and i is the imaginary unit. The space $\mathbb{R}^3$ is divided by the planar surface, $\partial\mathbb{N} = \{(\mathbf{x}_T, x_3) | \mathbf{x}_T \in \mathbb{R}^2, x_3 = x_3^{t1}\}$, into an upper half-space $\mathbb{N}^u$ and a lower half-space $\mathbb{N}^1$ (Fig. 1). We consider inside $\mathbb{N}^u$ the reference and monitor source distributions at $\mathbf{x}' = \mathbf{x}^R$ and $\mathbf{x}' = \mathbf{x}^S$, respectively. We define, omitting the ω-dependency, the following interaction integral,

$$\hat{I}^{conv}(x_3^{t1};\mathbf{x}^R,\mathbf{x}^S) \stackrel{def}{=} \int_{\mathbf{x}_T \in \mathbb{R}^2} [\hat{v}_3^{(1)}(\mathbf{x}_T, x_3^{t1};\mathbf{x}^R)\hat{p}^{(2)}(\mathbf{x}_T, x_3^{t1};\mathbf{x}^S) - \hat{p}^{(1)}(\mathbf{x}_T, x_3^{t1};\mathbf{x}^R)\hat{v}_3^{(2)}(\mathbf{x}_T, x_3^{t1};\mathbf{x}^S)]d\mathbf{x}_T \quad , \tag{3}$$

(Fokkema et al., 1999; Dillen et al., 2000; Dillen, 2000). The integration is with respect to the transverse coordinate $\mathbf{x}_T$, at x_3^{t1}. The boundary integral follows from the application of the acoustic reciprocity theorem of the time-convolution type (Fokkema and van den Berg, 1993). The reciprocity theorem equates the boundary integral to two volume integrals over $\mathbb{N}^u$, one in terms of the temporal contrasts between the medium parameters, and the other in terms of the reference and monitor sources. In case the reference and monitor media are identical in $\mathbb{N}^u$ the latter volume integral remains. Considering point sources the boundary integral is then represented by a difference wave field (Fokkema et al., 1999). In Wapenaar et al. (2000), applications of a similar boundary integral in terms of one-way wave fields are presented. In the following section, the boundary integral of Eq. (3) is evaluated numerically.

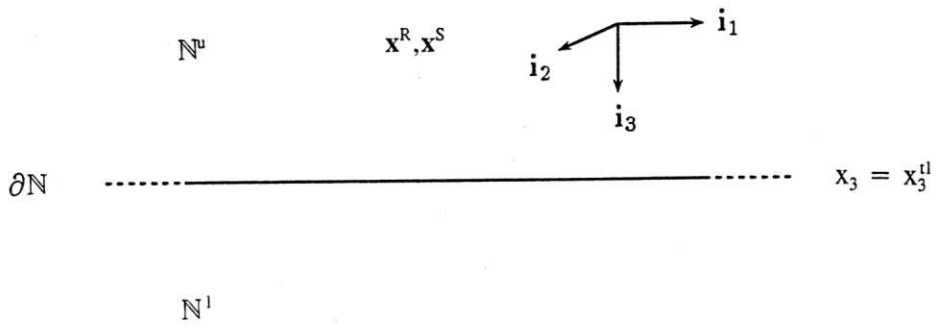

Fig. 1. Time-lapse configuration with source positions in upper half-space $\mathbb{N}^u$.

NUMERICAL EXAMPLE 1

We consider the two-dimensional model shown in Fig. 2(a), with coordinate vector $\mathbf{x} = (x_1,x_3)$, in which x_1 denotes the lateral position in terms of source and receiver offset from the origin, and x_3 denotes depth (no x_2 dependency). The wave fields are calculated and displayed in the time domain. The reference and monitor velocities and densities are given in Table 1. The reference and monitor sources are placed at the top of the model at 0 m depth. The monitor source offset is taken at 0 m, whereas the reference sources are taken at various offsets, such that $I^{conv}(x_3^{tl};\mathbf{x}^R,\mathbf{x}^S)$ produces a single gather with traces corresponding to the different reference source coordinates. The receivers for both experiments are placed at 0 m depth, at offsets covering the entire model. Fig. 2(b) shows a difference gather obtained by subtracting a single reference shot-gather from a single monitor shot-gather, with both shots placed

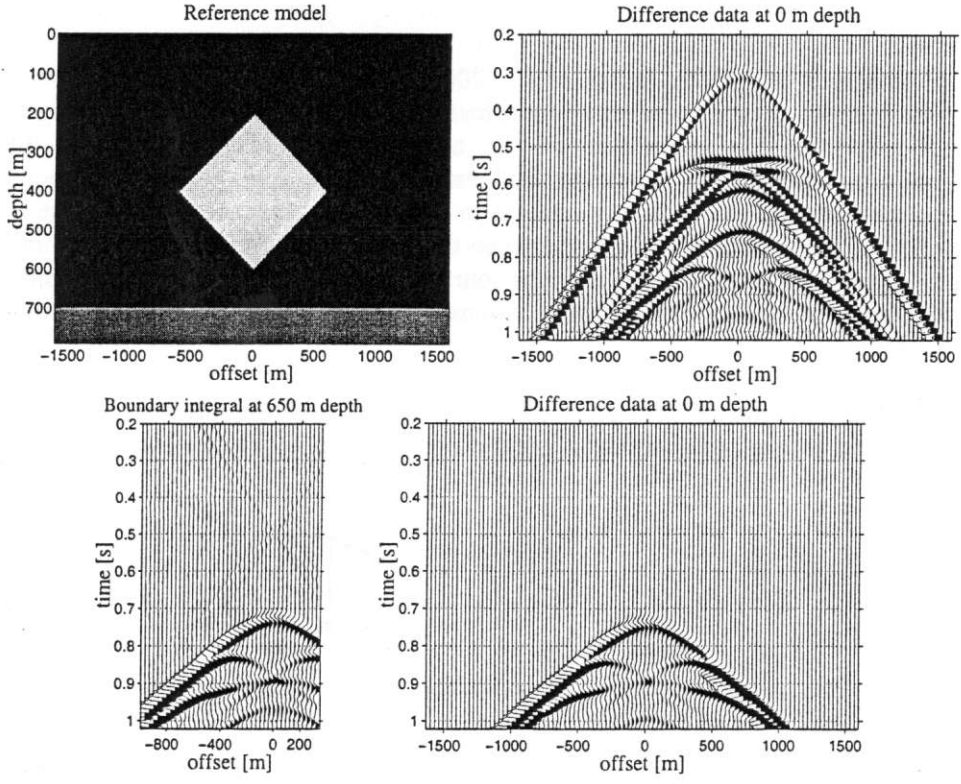

Fig. 2. (a) Model containing a diamond-shaped object, embedded in a background medium, and a lower layer. Temporal contrast in diamond-shaped object and lower layer. (b) Difference wave field evaluated at $x_3 = 0$ m depth for a range of offsets covering the model. (c) Interaction integral of Eq. (3) at $x_3^{tl} = 650$ m. (d) Difference wave field at $x_3 = 0$ m, no temporal contrasts for $x_3 < 650$ m.

at the origin. We proceed by computing the interaction integral of Eq. (3) at x_3^{tl} = 650 m, i.e., between the diamond-shaped object and the lower layer, for (x_1^S,x_3^S) = (0,0) m, and x_1^R ranging over various offsets, and x_3^R = 0 m. The result is shown in Fig. 2(c), for a selected range of x_1^R values. Next, the monitor model is changed such that it equals the reference model for $x_3 < 650$ m, according to Table 2, thereby eliminating the temporal contrast in the diamond-shaped object and retaining the temporal contrast in the lower layer. The resulting difference gather, using the same source/receiver parameters with which Fig. 2(b) is obtained, is shown in Fig. 2(d). The difference reflections associated with the temporal contrast in the diamond-shaped object, visible in Fig. 2(b) have disappeared in Fig. 2(d). Note the similarity of Fig. 2(d) with Fig. 2(c), thereby indicating that the interaction integral can be identified with a difference wave field which shows no temporal contrast above the interaction depth. In the following two sections this apparent vanishing of difference reflections in the boundary integral gather is investigated analytically.

Table 1. Reference and monitor velocities and densities, $c^{(1)}$, $\rho^{(1)}$, $c^{(2)}$ and $\rho^{(2)}$.

	$c^{(1)}$ [m/s]	$\rho^{(1)}$ [kg/m^3]	$c^{(2)}$ [m/s]	$\rho^{(2)}$ [kg/m^3]
background	1800	1500	1800	1500
diamond-shaped object	2500	2000	2700	2200
lower layer	2700	2300	2900	2400

Table 2. Updated reference and monitor velocities and densities, $c^{(1)}$,$\rho^{(1)}$, $c^{(2)}$ and $\rho^{(2)}$, no temporal contrasts for $x_3 < 650$ m.

	$c^{(1)}$ [m/s]	$\rho^{(1)}$ [kg/m^3]	$c^{(2)}$ [m/s]	$\rho^{(2)}$ [kg/m^3]
background	1800	1500	1800	1500
diamond-shaped object	2500	2000	2500	2000
lower layer	2700	2300	2900	2400

WAVE FIELD DECOMPOSITION

In $\mathbb{R}^3$ the *background* medium parameters $\{\rho^b,\kappa^b\}$, are defined with respect to the actual medium parameters $\{\rho,\kappa\}$, through the perturbation $\{\delta\rho,\delta\kappa\}$, according to

$$\{\rho,\kappa\} = \{\rho^b,\kappa^b\} \quad , \qquad \text{in } \mathbb{N}^u \quad , \tag{4}$$

$$\{\rho,\kappa\} = \{\rho^b,\kappa^b\} + \{\delta\rho,\delta\kappa\} \quad , \quad \text{in } \mathbb{N}^l \quad , \tag{5}$$

(see Fig. 1). Inside $\mathbb{N} = \{(\mathbf{x}_T,x_3)\,|\,\mathbf{x}_T \in \mathbb{R}^2,\ \max(x_3^R,x_3^S) \leq x_3 \leq x_3^{tl}\}$ the actual wave field $\{\hat{p},\hat{v}_3\}$, also denoted as the *total* wave field, is decomposed into a *down-going* wave field $\{\hat{p}^d,\hat{v}_3^d\}$, and an *up-going* wave field $\{\hat{p}^u,\hat{v}_3^u\}$, as

$$\hat{p} = \hat{p}^d + \hat{p}^u \quad , \tag{6}$$

$$\hat{v}_3 = \hat{v}_3^d + \hat{v}_3^u \quad , \tag{7}$$

with

$$\hat{v}_3^d = \hat{Y}^b\hat{p}^d \quad , \tag{8}$$

$$\hat{v}_3^u = -\hat{Y}^b\hat{p}^u \quad , \tag{9}$$

(Dillen, 2000). The operators $\pm\hat{Y}^b$ are *Dirichlet-to-Neumann* (D-t-N) operators which map a pressure function to the longitudinal component of a particle velocity function. The wave field decomposition of Eqs. (6) and (7) follows from a particular normalization of the incident and scattered wave fields associated with the perturbation of Eqs. (4) and (5). The wave field directions 'down' and 'up' are determined globally with respect to $\mathbb{N}$, i.e., locally, inside $\mathbb{N}$, the directionality is undetermined. In Haines and de Hoop (1996) a similar decomposition is implemented, in terms of curvilinear coordinates, for the case of internal wave fields inside the scattering domain. For the *single-layer potential* operator $\hat{S}^b$, given by

$$\hat{S}^b f(\mathbf{x}_T,x_3) = 2 \fint_{x_T' \in \mathbb{R}^2} \hat{G}^{q,b}(\mathbf{x}_T,x_3;\mathbf{x}_T',x_3) f(\mathbf{x}_T',x_3) d\mathbf{x}_T' \quad , \tag{10}$$

with $f \in L^2(\mathbb{R}^2)$, and $\hat{G}^{q,b}$ being the monopole Green's function with respect to the background medium, one can show that

$$\hat{Y}^b = (\hat{S}^b)^{-1} \quad . \tag{11}$$

The integral symbol in Eq. (10) signifies a Cauchy principal value integral, in which the integration is over the pertaining boundary, with the symmetric exclusion of the singular point (Colton and Kress, 1983). Causality of the down- and up-going wave field components $\hat{p}^d$ and $\hat{p}^u$, yielding radiation conditions at infinity, gives symmetry for the D-t-N operator with respect to a bilinear form of scalar-valued functions $f \in L^2(\mathbb{R}^2)$ (Dillen, 2000), expressed as

$$\hat{Y}^b = (\hat{Y}^b)^t \quad . \tag{12}$$

Analogous to the previous equations one can obtain a D-t-N operator for the total wave field as

$$\hat{v}_3 = \hat{Y}\hat{p} \quad , \tag{13}$$

with

$$\hat{Y} = \hat{S}^{-1} \quad \text{and} \quad \hat{Y} = \hat{Y}^t \quad , \tag{14}$$

and with the single layer potential given by

$$\hat{S}g(\mathbf{x}_T,x_3) = 2 \oint_{x_T' \in \mathbb{R}^2} \hat{G}^q(\mathbf{x}_T,x_3;\mathbf{x}_T',x_3)g(\mathbf{x}_T',x_3)d\mathbf{x}_T' \quad , \tag{15}$$

with $g \in L^2(\mathbb{R}^2)$. Observe that the Green's function $\hat{G}^q$ in this last equation is given with respect to the actual medium in contradistinction to $\hat{G}^{q,b}$ in Eq. (10), which is given with respect to the background medium [see Eqs. (4) and (5)]. Associated with the wave field decomposition of Eqs. (6) to (9) we can derive the following reflection operator,

$$\hat{p}^u = \hat{R}\hat{p}^d \quad , \tag{16}$$

with

$$\hat{R} = (\hat{Y}^b + \hat{Y})^{-1}(\hat{Y}^b - \hat{Y}) \quad . \tag{17}$$

The reflection operator is a measure for the contrast in the D-t-N operators of Eqs. (11) and (14). In the following section we derive a time-lapse difference reflection operator for the case of equal background media.

EQUAL BACKGROUND MEDIA

The boundary integral (3) is rewritten to matrix-vector form, according to

$$\hat{I}^{conv}(x_3^{tl};\mathbf{x}^R,\mathbf{x}^S) = \int_{x_T \in \mathbb{R}^2} \begin{pmatrix} \hat{p}^{(1)} \\ \\ \hat{v}_3^{(1)} \end{pmatrix}^t (\mathbf{x}_T,x_3^{tl};\mathbf{x}^R)\, \mathbf{J} \begin{pmatrix} \hat{p}^{(2)} \\ \\ \hat{v}_3^{(2)} \end{pmatrix} (\mathbf{x}_T,x_3^{tl};\mathbf{x}^S)d\mathbf{x}_T \quad . \tag{18}$$

The superscript ^{t} denotes the transpose operation. The matrix $\mathbf{J}$ in this last equation,

$$\mathbf{J} = \begin{pmatrix} O & -I \\ I & O \end{pmatrix} , \tag{19}$$

is the *standard alternating* matrix, and O and I are the scalar null and identity operators, respectively. Substituting Eqs. (6) to (9), taken with respect to the reference and monitor states, into Eq. (18) yields

$$\hat{I}^{\text{conv}}(x_3^{\text{tl}};\mathbf{x}^{\text{R}},\mathbf{x}^{\text{S}}) = \int_{x_{\text{T}}\in\mathbb{R}^2} \begin{pmatrix} \hat{p}^{\text{d},(1)} \\ \hat{p}^{\text{u},(1)} \end{pmatrix}^{\text{t}} (\mathbf{x}_{\text{T}},x_3^{\text{tl}};\mathbf{x}^{\text{R}})\, \hat{\mathbf{Y}}^{\text{b}} \begin{pmatrix} \hat{p}^{\text{d},(2)} \\ \hat{p}^{\text{u},(2)} \end{pmatrix} (\mathbf{x}_{\text{T}},x_3^{\text{tl}};\mathbf{x}^{\text{S}})\mathrm{d}\mathbf{x}_{\text{T}} \quad , \tag{20}$$

with the interaction matrix $\hat{\mathbf{Y}}^{\text{b}}$ given by

$$\hat{\mathbf{Y}}^{\text{b}} = \begin{pmatrix} -\hat{Y}^{\text{b},(2)} + \hat{Y}^{\text{b},(1)} & \hat{Y}^{\text{b},(2)} + \hat{Y}^{\text{b},(1)} \\ -\hat{Y}^{\text{b},(2)} - \hat{Y}^{\text{b},(1)} & \hat{Y}^{\text{b},(2)} - \hat{Y}^{\text{b},(1)} \end{pmatrix} \quad . \tag{21}$$

In this last equation we used, according to Eq. (12), the symmetry of the pertaining D-t-N operators. Observe that $\hat{\mathbf{Y}}^{\text{b}}$ is a symplectic operator, i.e.,

$$(\hat{\mathbf{Y}}^{\text{b}})^{\text{t}}\mathbf{J} + \mathbf{J}\hat{\mathbf{Y}}^{\text{b}} = \mathbf{O} \quad , \tag{22}$$

with $\mathbf{O}$ being the (2×2)-matrix null operator. Suppose that there are no temporal contrasts in the medium parameters ρ and κ above the interaction depth x_3^{tl}, i.e., inside the upper half-space $\mathbb{N}^{\text{u}}$ (Fig. 1). Hence, according to Eqs. (4) and (5) we consider equal background media. Then, the interaction matrix becomes skew-symmetric, expressed as

$$\hat{\mathbf{Y}}^{\text{b}}\big|_{\{\rho^{\text{b},(1)},\kappa^{\text{b},(1)}\} = \{\rho^{\text{b},(2)},\kappa^{\text{b},(2)}\}} = \begin{pmatrix} O & 2\hat{Y}^{\text{b}} \\ -2\hat{Y}^{\text{b}} & O \end{pmatrix} \quad , \tag{23}$$

with

$$\hat{Y}^{\text{b}} = \hat{Y}^{\text{b},(1)} = \hat{Y}^{\text{b},(2)} \quad . \tag{24}$$

Taking identical background media in Eq. (20), using Eq. (23), yields

$$\begin{aligned} &\hat{I}^{\text{conv}}(x_3^{\text{tl}};\mathbf{x}^{\text{R}},\mathbf{x}^{\text{S}})\big|_{\{\rho^{\text{b},(1)},\kappa^{\text{b},(1)}\} = \{\rho^{\text{b},(2)},\kappa^{\text{b},(2)}\}} \\ &\quad = 2\int_{x_{\text{T}}\in\mathbb{R}^2} [\hat{p}^{\text{d},(1)}(\mathbf{x}_{\text{T}},x_3^{\text{tl}};\mathbf{x}^{\text{R}})\hat{Y}^{\text{b}}\,\hat{p}^{\text{u},(2)}(\mathbf{x}_{\text{T}},x_3^{\text{tl}};\mathbf{x}^{\text{S}}) \\ &\qquad - \hat{p}^{\text{u},(1)}(\mathbf{x}_{\text{T}},x_3^{\text{tl}};\mathbf{x}^{\text{R}})\hat{Y}^{\text{b}}\,\hat{p}^{\text{d},(2)}(\mathbf{x}_{\text{T}},x_3^{\text{tl}};\mathbf{x}^{\text{S}})]\mathrm{d}\mathbf{x}_{\text{T}} \quad . \end{aligned} \tag{25}$$

Comparing Eq. (20) with Eq. (25), the latter equation only involves paired interactions of wave fields traveling in opposite directions. Using Eqs. (16) and (17) we obtain the reference and monitor reflection operations

$$\hat{p}^{u,(1)} = \hat{R}^{(1)}\hat{p}^{d,(1)} \quad , \tag{26}$$

$$\hat{p}^{u,(2)} = \hat{R}^{(2)}\hat{p}^{d,(2)} \quad , \tag{27}$$

with

$$\hat{R}^{(1)} = (\hat{Y}^{b} + \hat{Y}^{(1)})^{-1}(\hat{Y}^{b} - \hat{Y}^{(1)}) \quad , \tag{28}$$

$$\hat{R}^{(2)} = (\hat{Y}^{b} + \hat{Y}^{(2)})^{-1}(\hat{Y}^{b} - \hat{Y}^{(2)}) \quad . \tag{29}$$

Substituting Eqs. (26) and (27) into Eq. (25), and using the symmetry of $\hat{Y}^{b}$, yields

$$\begin{aligned} &\hat{I}^{conv}(x_3^{tl};\mathbf{x}^{R},\mathbf{x}^{S})\big|_{\{\rho^{b,(1)},\kappa^{b,(1)}\} = \{\rho^{b,(2)},\kappa^{b,(2)}\}} \\ &\quad = 2\int_{\mathbf{x}_T\in\mathbb{R}^2} [\hat{p}^{d,(1)}(\mathbf{x}_T,x_3^{tl};\mathbf{x}^{R})\hat{Y}^{b}\hat{R}^{(2)}\hat{p}^{d,(2)}(\mathbf{x}_T,x_3^{tl};\mathbf{x}^{S}) \\ &\quad - \hat{Y}^{b}\hat{R}^{(1)}\hat{p}^{d,(1)}(\mathbf{x}_T,x_3^{tl};\mathbf{x}^{R})\hat{p}^{d,(2)}(\mathbf{x}_T,x_3^{tl};\mathbf{x}^{S})]d\mathbf{x}_T \quad . \end{aligned} \tag{30}$$

Assuming equality of the reference and monitor medium parameters throughout $\mathbb{R}^3$, one can show, by applying causality radiation conditions at infinity, that we have

$$\begin{aligned} &\hat{I}^{conv}(x_3^{tl};\mathbf{x}^{R},\mathbf{x}^{S})\big|_{\{\rho^{(1)},\kappa^{(1)}\} = \{\rho^{(2)},\kappa^{(2)}\}} \\ &\quad = 2\int_{\mathbf{x}_T\in\mathbb{R}^2} [\hat{p}^{d,(1)}(\mathbf{x}_T,x_3^{tl};\mathbf{x}^{R})\hat{Y}^{b}\hat{R}\hat{p}^{d,(2)}(\mathbf{x}_T,x_3^{tl};\mathbf{x}^{S}) \\ &\quad - \hat{Y}^{b}\hat{R}\hat{p}^{d,(1)}(\mathbf{x}_T,x_3^{tl};\mathbf{x}^{R})\hat{p}^{d,(2)}(\mathbf{x}_T,x_3^{tl};\mathbf{x}^{S})]d\mathbf{x}_T = 0 \quad , \end{aligned} \tag{31}$$

in which

$$\hat{R} = \hat{R}^{(1)} = \hat{R}^{(2)} \quad . \tag{32}$$

Hence, we obtain the symmetry

$$\hat{Y}^{b}\hat{R} = (\hat{Y}^{b}\hat{R})^{t} \quad . \tag{33}$$

Because the reference and monitor down-going wave fields are governed by the same background media we can use the monopole Green's functions, introduced in Eq. (10), as

$$\hat{p}^{d,(1)} = \hat{q}^{(1)}\hat{G}^{q,b} \quad , \tag{34}$$

$$\hat{p}^{d,(2)} = \hat{q}^{(2)}\hat{G}^{q,b} \quad . \tag{35}$$

Because the symmetry (33) must hold for any medium, Eq. (30) can be written, using Eqs. (34) and (35), and again using symmetry (12), as

$$\hat{I}^{\text{conv}}(x_3^{\text{tl}};\mathbf{x}^{\text{R}},\mathbf{x}^{\text{S}})\,|_{\{\rho^{\text{b},(1)},\kappa^{\text{b},(1)}\}\,=\,\{\rho^{\text{b},(2)},\kappa^{\text{b},(2)}\}}$$

$$= 2\hat{q}^{(1)}\hat{q}^{(2)} \int_{\mathbf{x}_{\text{T}}\in\mathbb{R}^2} \Delta\hat{R}\hat{G}^{\text{q,b}}(\mathbf{x}_{\text{T}},x_3^{\text{tl}};\mathbf{x}^{\text{R}})\hat{Y}^{\text{b}}\hat{G}^{\text{q,b}}(\mathbf{x}_{\text{T}},x_3^{\text{tl}};\mathbf{x}^{\text{S}})\text{d}\mathbf{x}_{\text{T}} \quad , \tag{36}$$

in which the difference reflection operator is given by

$$\Delta\hat{R}\,|_{\{\rho^{\text{b},(1)},\kappa^{\text{b},(1)}\}\,=\,\{\rho^{\text{b},(2)},\kappa^{\text{b},(2)}\}} = \hat{R}^{(2)} - \hat{R}^{(1)} \quad . \tag{37}$$

Hence, by assuming equal background media, i.e., no temporal contrast between the reference and monitor media for $x_3 < x_3^{\text{tl}}$, we can identify with the boundary integral $\hat{I}^{\text{conv}}$ a difference reflection operator. The propagation part is governed by two background Green's function, with sources in $\mathbf{x}^{\text{R}}$ and $\mathbf{x}^{\text{S}}$, respectively. This difference reflection operator models difference reflections from temporal contrasts located at $x_3 > x_3^{\text{tl}}$.

One can show, using the reciprocity theorem, for the time-lapse wave fields of Eqs. (1) and (2), assuming equal background media, and with a non-vanishing $\hat{q}$ source and a vanishing $\hat{f}_k$ source, that the boundary integral is equivalent to a difference wave field (Fokkema et al., 1999),

$$\hat{I}^{\text{conv}}(x_3^{\text{tl}};\mathbf{x}^{\text{R}},\mathbf{x}^{\text{S}})\,|_{\{\rho^{\text{b},(1)},\kappa^{\text{b},(1)}\}\,=\,\{\rho^{\text{b},(2)},\kappa^{\text{b},(2)}\}}$$

$$= \hat{q}^{(1)}\hat{p}^{(2)}(\mathbf{x}^{\text{R}};\mathbf{x}^{\text{S}}) - \hat{q}^{(2)}\hat{p}^{(1)}(\mathbf{x}^{\text{R}};\mathbf{x}^{\text{S}}) \quad . \tag{38}$$

In the derivation of this last equation source-receiver reciprocity is used for the reference wave field such that this wave field has the same source-receiver configuration as the monitor wave field. A numerical example of the boundary integral of Eq. (36), computed using the difference wave field of Eq. (38), is shown in Fig. 2(d). The associated difference reflections are described by $\Delta\hat{R}$ of Eq. (37).

UNEQUAL BACKGROUND MEDIA

We arrived at a representation of the boundary integral in terms of a difference reflection and a difference wave field by assuming point-like equality of ρ^{b} and κ^{b} for $x_3 < x_3^{\text{tl}}$. This assumption leads to skew-symmetry of the interaction matrix $\hat{\mathbf{Y}}^{\text{b}}$, as is shown in Eq. (23). However, a sufficient condition for skew-symmetry of $\hat{\mathbf{Y}}^{\text{b}}$ is the equality of the reference and monitor background D-t-N operators $\hat{\mathbf{Y}}^{\text{b},(1)}$ and $\hat{\mathbf{Y}}^{\text{b},(2)}$. This condition is not necessarily a point-like equality of the two background media but is governed by an integral

as given in Eq. (10). Hence, it involves some averaging of the reference and monitor parameters ρ^b and κ^b with respect to the transverse direction. Exploiting this weak property, and the fact that the interaction operator $\hat{\mathbf{Y}}^b$ is symplectic, according to Eq. (22), we can transform $\hat{\mathbf{Y}}^b$ of Eq. (21) to skew-symmetric form by employing a symplectic eigenvalue decomposition according to

$$\hat{\mathbf{Y}}^b\hat{\mathbf{Q}} = \hat{\mathbf{Q}}\hat{\mathbf{Y}}^{tl} \quad , \tag{39}$$

(Abraham et al., 1978; Dillen, 2000). The skew-symmetric interaction matrix $\hat{\mathbf{Y}}^{tl}$ is given by

$$\hat{\mathbf{Y}}^{tl} = \begin{pmatrix} O & 2\hat{Y}^{tl} \\ -2\hat{Y}^{tl} & O \end{pmatrix} \quad , \tag{40}$$

with the symplectic eigenvalue operator

$$\hat{Y}^{tl} = (\hat{Y}^{b,(2)}\,\hat{Y}^{b,(1)})^{1/2} \quad . \tag{41}$$

The square root of the operator in this last equation is taken as

$$\hat{Y}^{tl}\hat{Y}^{tl} = \hat{Y}^{b,(2)}\,\hat{Y}^{b,(1)} \quad . \tag{42}$$

The matrix of symplectic eigenvectors is given by

$$\hat{\mathbf{Q}} = \tfrac{1}{2}\begin{pmatrix} I + (\hat{Y}^{b,(1)})^{1/2}(\hat{Y}^{b,(2)})^{-1/2} & I - (\hat{Y}^{b,(1)})^{1/2}(\hat{Y}^{b,(2)})^{-1/2} \\ I - (\hat{Y}^{b,(1)})^{1/2}(\hat{Y}^{b,(2)})^{-1/2} & I + (\hat{Y}^{b,(1)})^{1/2}(\hat{Y}^{b,(2)})^{-1/2} \end{pmatrix} \quad , \tag{43}$$

in which the square roots are taken according to Eq. (42). On the new symplectic basis we obtain the following wave field constituents

$$\begin{pmatrix} \hat{p}^{d,(1)'} \\ \hat{p}^{u,(1)'} \end{pmatrix} = \hat{\mathbf{Q}}\begin{pmatrix} \hat{p}^{d,(1)} \\ \hat{p}^{u,(1)} \end{pmatrix} \quad \text{and} \quad \begin{pmatrix} \hat{p}^{d,(2)'} \\ \hat{p}^{u,(2)'} \end{pmatrix} = \hat{\mathbf{Q}}^{-1}\begin{pmatrix} \hat{p}^{d,(2)} \\ \hat{p}^{u,(2)} \end{pmatrix} \quad . \tag{44}$$

Using the latter transformation and Eqs. (6) to (9), applied to either the reference or the monitor state, one can show that both the reference and monitor wave fields can be decomposed according to

$$\hat{p} = \hat{p}^{d'} + \hat{p}^{u'} \quad , \tag{45}$$

$$\hat{v}_3 = \hat{v}_3^{d'} + \hat{v}_3^{u'} \quad , \tag{46}$$

with

$$\hat{v}_3^{d'} = \hat{Y}^{tl}\hat{p}^{d'} \quad , \tag{47}$$

$$\hat{v}_3^{u'} = -\hat{Y}^{tl}\hat{p}^{u'} \quad . \tag{48}$$

Implementing the decomposition of Eq. (39) into Eq. (20) yields

$$\begin{aligned}\hat{I}^{conv}(x_3^{tl};\mathbf{x}^R,\mathbf{x}^S) \\ = 2\int_{x_T\in\mathbb{R}^2} [\hat{p}^{d,(1)'}(\mathbf{x}_T,x_3^{tl};\mathbf{x}^R)\hat{Y}^{tl}\hat{p}^{u,(2)'}(\mathbf{x}_T,x_3^{tl};\mathbf{x}^S) \\ - \hat{p}^{u,(1)'}(\mathbf{x}_T,x_3^{tl};\mathbf{x}^R)\hat{Y}^{tl}\hat{p}^{d,(2)'}(\mathbf{x}_T,x_3^{tl};\mathbf{x}^S)]d\mathbf{x}_T \quad ,\end{aligned} \tag{49}$$

in which the primed wave field constituents are given with respect to the new symplectic basis according to Eq. (44). Observe that this last equation has the same form as Eq. (25), i.e., we retained paired interactions of wave fields travelling in opposite directions. For the special case of equal background media $\hat{Y}^{tl}$ of Eq. (40) becomes $\hat{Y}^{b}$ of Eq. (23). Also, for this case $\hat{Q}$ of Eq. (43) becomes the (2×2) identity operator and hence the primed wave field constituents of Eq. (44) equal the unprimed ones. Consequently, the representation of Eq. (49) becomes Eq. (25).

Analogously to Eqs. (26) and (27) we obtain the following reflection operations

$$\hat{p}^{u,(1)'} = \hat{R}^{tl,(1)}\hat{p}^{d,(1)'} \quad , \tag{50}$$

$$\hat{p}^{u,(2)'} = \hat{R}^{tl,(2)}\hat{p}^{d,(2)'} \quad , \tag{51}$$

with

$$\hat{R}^{tl,(1)} = (\hat{Y}^{tl} + \hat{Y}^{(1)})^{-1}(\hat{Y}^{tl} - \hat{Y}^{(1)}) \quad , \tag{52}$$

$$\hat{R}^{tl,(2)} = (\hat{Y}^{tl} + \hat{Y}^{(2)})^{-1}(\hat{Y}^{tl} - \hat{Y}^{(2)}) \quad . \tag{53}$$

These latter reflection operators have the same form as the ones in Eqs. (28) and (29). We define the following Green's functions

$$\hat{p}^{d,(1)'} = \hat{q}^{(1)}\hat{G}^{q,tl,(1)} \quad , \tag{54}$$

$$\hat{p}^{d,(2)'} = \hat{q}^{(2)}\hat{G}^{q,tl,(2)} \quad . \tag{55}$$

Observe that in these last two equations the Green's functions are unequal, whereas the Green's functions in Eqs. (34) and (35) are equal. Performing the same analysis which follows Eq. (25), for the case of equal background media,

one obtains for the general case of possibly unequal background media

$$\hat{I}^{conv}(x_3^{tl};\mathbf{x}^R,\mathbf{x}^S)$$

$$= 2\hat{q}^{(1)}\hat{q}^{(2)} \int_{\mathbf{x}_T\in\mathbb{R}^2} \Delta\hat{R}^{tl}\,\hat{G}^{q,tl,(1)}(\mathbf{x}_T,x_3^{tl};\mathbf{x}^R)\hat{Y}^{tl}\,\hat{G}^{q,tl,(2)}(\mathbf{x}_T,x_3^{tl};\mathbf{x}^S)d\mathbf{x}_T \quad , \tag{56}$$

in which the difference reflection is given by

$$\Delta\hat{R}^{tl} = \hat{R}^{tl,(2)} - \hat{R}^{tl,(1)} \quad . \tag{57}$$

Hence, analogously to Eq. (36), also for the general case of unequal background media, i.e., possible temporal contrasts between the reference and monitor media for $x_3 < x_3^{tl}$, we can identify with the boundary integral $\hat{I}^{conv}$ a difference reflection operator. The propagation part is governed by two unequal Green's functions, with sources in $\mathbf{x}^R$ and $\mathbf{x}^S$, respectively. The inequality of the background media does not produce associated difference reflections in a I^{conv}-gather, because these, according to Eq. (17), are generated by a temporal contrast in the D-t-N operator only. The above analysis shows that the reference and monitor states share, on the new symplectic basis, the same D-t-N operator $\hat{Y}^{tl}$ for $x_3 < x_3^{tl}$. Therefore, as was shown in Fig. 2(c), the application of the boundary integral eliminates difference reflections for $x_3 < x_3^{tl}$.

In Dillen et al. (2000) it is shown that, for the general case of unequal background media, the boundary integral of Eq. (3) represents a difference wave field, originating from temporal contrast sources below the boundary, at which this integral is evaluated. This difference wave field is however different from Eq. (38) but has the same appearance, as was shown by Figs. 2(c) and 2(d). We can regard the equality of the boundary integral with a difference wave field in the same way as the Helmholtz integral, or the Kirchhoff integral in case of the time-domain, can represent a scattered wave field from spatial contrast sources below the evaluation depth. Recursive computation of the boundary integral eliminates difference reflections above the interaction depth, giving a basis for pre-stack temporal contrast imaging and inversion schemes, analogous to implementations of the Helmholtz integral in inverse scattering theory.

NUMERICAL EXAMPLE 2

To illustrate the recursive temporal contrast elimination scheme consider the model of Fig. 3(a) which consists of 6 layers. Using this configuration reference and monitor wave speeds, $c^{(1)}$ and $c^{(2)}$, and densities, $\rho^{(1)}$ and $\rho^{(2)}$, are assigned according to Table 3. Wave fields were generated using finite differences. Time-lapse changes are modeled in layer 1, in which the source and receivers are placed, such that non-repeatability of the time-lapse experiments

is simulated, and in layer 3 and 5. In Fig. 3(b) the difference wave field is shown, obtained by placing the source and receiver array at 0 m depth. In this figure a difference direct wave, associated with the time-lapse changes in layer 1, and several difference reflections, associated with the time-lapse changes in layer 1, 3 and 5, are observable. Calculating I^{conv} of Eq. (3) at $x_3^{tl} = 80$ m depth, i.e., halfway layer 1, we obtain Fig. 4(a). It appears that the difference direct wave associated with time-lapse contrasts for $x_3 < 80$ m has disappeared, as compared to Fig. 3(b). Hence, differences in the medium parameters in the source and receiver domains are cancelled in the I^{conv}-gather of Fig. 4(a). In this way, non-repeatability of a time-lapse measurement, associated with time-lapse differences in the medium parameters in the neighbourhood of source and receiver, is eliminated. For $x_3 < 80$ m we obtain a parameterization in terms of $\hat{Y}^{tl}$ of Eq. (41). Therefore, a difference reflection is introduced at the interaction depth $x_3^{tl} = 80$ m, as compared to Fig. 3(b) in which this difference reflection does not appear. The time shifts of the difference reflections in Fig. 3(b) depend on the time-lapse contrasts for $x_3 < 80$ m. In Fig. 4(a) the time-shifts of the difference reflections induced by the time-lapse contrasts for $x_3 < 80$ m have disappeared. Also the amplitudes of the difference reflections in Fig. 4(a) are corrected, as compared to Fig. 3(b), such that their dependencies on the temporal contrasts for $x_3 < 80$ m are cancelled. Hence, the corrective action of the interaction integral is both kinematically as well as dynamically valid. In Figs. 4(b) to 4(d) the interaction integral I^{conv} is calculated at $x_3^{tl} = 164$, 256 and 404 m depths, i.e., just below layer 1, just above layer 3, and just below layer 3, respectively [see Fig. 3(a)].

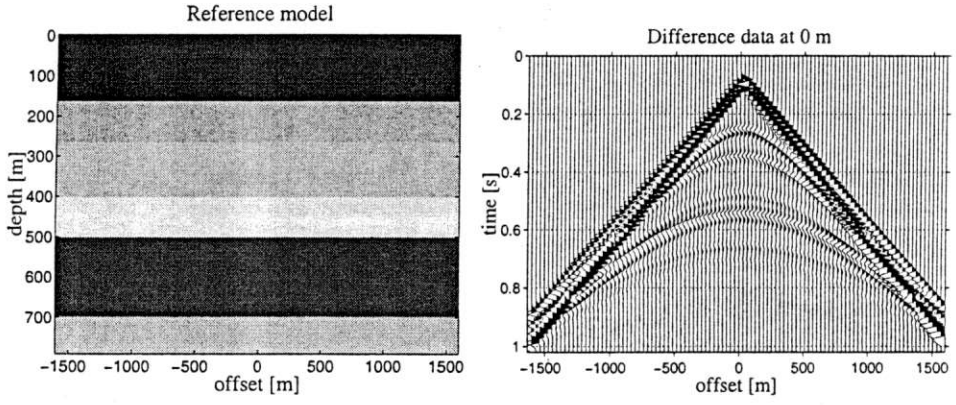

Fig. 3. (a) Layered model with time-lapse differences in first, third and fifth layer. (b) Difference wave field at the surface.

Table 3. Reference and monitor velocities and densities, $c^{(1)}$, $\rho^{(1)}$ and $c^{(2)}$ and $\rho^{(2)}$.

layer	$c^{(1)}$ [m/s]	$\rho^{(1)}$ [kg/m^3]	$c^{(2)}$ [m/s]	$\rho^{(2)}$ [kg/m^3]
1	1800	1500	2000	1600
2	2100	1700	2100	1700
3	2200	1800	2400	1900
4	2500	2000	2500	2000
5	3000	2400	3200	2500
6	2700	2300	2700	2300

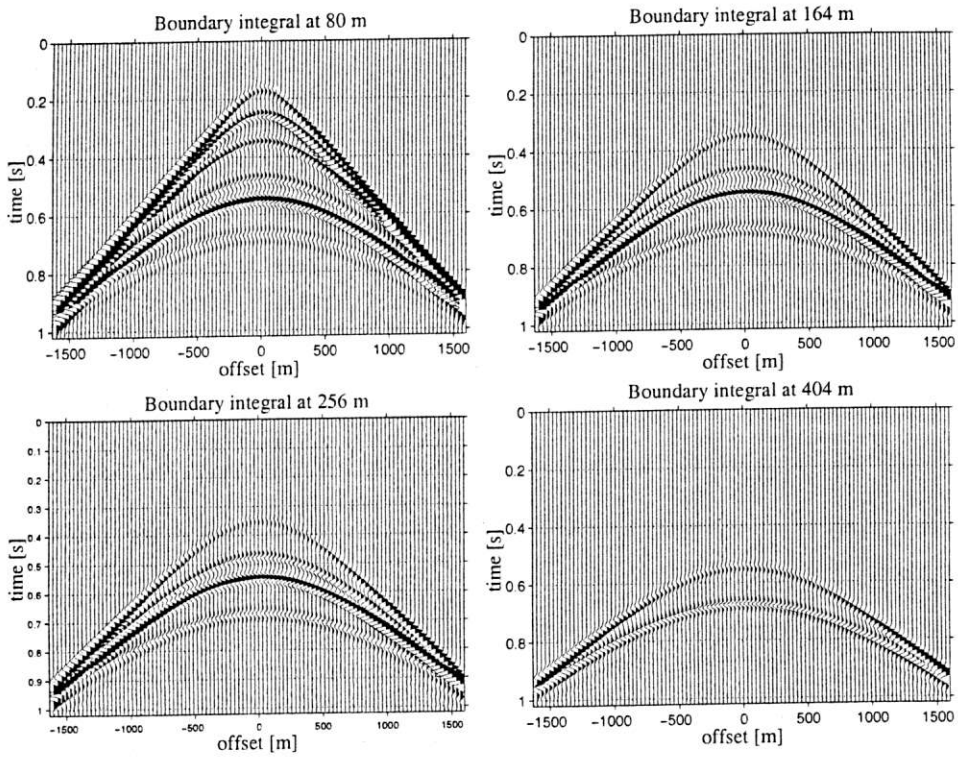

Fig. 4. (a) Interaction integral of Eq. (3) at $x_3^{tl} = 80$ m, (b) at $x_3^{tl} = 164$ m, (c) at $x_3^{tl} = 256$ m, and (d) at $x_3^{tl} = 404$ m.

One observes that in Fig. 4(b) the time-shifts and amplitudes of the difference reflections are such that these appear to be independent of the temporal contrasts in layer 1, and depend only on the temporal contrasts in layer 3 and 5. Fig. 4(c) is the same as Fig. 4(b), showing that I^{conv} is an invariant in a domain (in this case layer 2) in which no time-lapse changes have occurred. In Fig. 4(d) the difference reflections are associated with the time-lapse contrast in layer 5 only, and are independent of the time-lapse contrasts in layer 1 and layer 3. Observe that, in Fig. 4(d), the first difference reflection, associated with the top of layer 5, is a pure amplitude difference, involving no time-shift, in contradistinction to the same difference reflection in Figs. 3(b) and 4(a) to 4(c). This difference reflection of the top of layer 5 in Fig. 3(b) contains the sum of the time-shifts induced by the temporal contrasts in layer 1 and 3, whereas the same difference reflection in Fig. 4(c) contains the time-shift induced by the temporal contrast in layer 3.

DISCUSSION

Computing the interaction integral recursively, according to Eq. (3), as was shown in the previous examples, one can device an inversion scheme based on the minimization of phase shifts and difference amplitudes. To do so, the reference and monitor wave fields in the integrand of the boundary integral are computed at the integration level as follows. First, the total reference and monitor wave fields, at the level of measurement, are decomposed into down- and up-going wave field constituents, by identifying the source wave fields, and subsequently subtracting these from the total wave field measurements. The down- and up-going wave fields are governed by the background medium parameters. Using these parameters the down- and up-going wave fields are, respectively, forward and backward propagated, to the integration level, and subsequently summed to obtain the total wave fields. This process is iterated to obtain the background medium parameters which minimise the difference reflections. Sufficient constraints have to be imposed to handle the non-uniqueness problem. This inversion would yield the time-lapse changes of the medium parameters above the integration level. A similar procedure is applied in Wapenaar et al. (2000) for a boundary integral in terms of one-way wave fields. Having obtained these medium parameters one can compute the kernel of the difference reflection from the boundary integral using Eq. (56). From the difference reflection kernel time-lapse perturbations in the compressibility and the density can be inferred for the medium below the level at which the boundary integral is evaluated. Using a suitable parameterization one could linearize this inversion, e.g., for small temporal contrasts, and carry out an AVO-type analysis.

In practice, the reference and monitor wave fields in the integrand of the boundary integral are determined using computational background media, based on partial and insufficient knowledge of the actual media. However, the interaction of two actual wave fields is considered. This in contradistinction to spatial scattering formalisms, in which an actual measurement wave field interacts with a smooth computational wave field. For this reason one may expect that with time-lapse seismic measurements a higher resolution can be attained than with single seismic measurements.

REFERENCES

Abraham, R. and Marsden, J.E., 1978. Foundations of Mechanics, 2nd Ed. The Benjamin/Cummings Publishing Company, Inc., New York.

Colton, D. and Kress, R., 1983. Integral Equation Methods in Scattering Theory. John Wiley and Sons, New York.

Dillen, M.W.P., Fokkema, J.T. and Wapenaar, C.P.A., 2000. Convolution type interaction of time-lapse acoustic wave fields. Expanded Abstr., 70th Ann. Internat. SEG Mtg., Calgary: 2381-2384.

Dillen, M.W.P., 2000. Time-lapse seismic monitoring of subsurface stress dynamics. Ph.D. thesis, Delft University of Technology, Delft.

Fokkema, J.T. and van den Berg, P.M., 1993. Seismic Applications of Acoustic Reciprocity. Elsevier Science Publishers, Amsterdam.

Fokkema, J.T., Wapenaar, C.P.A. and Dillen, M.W.P., 1999. Reciprocity theorems for time-lapse seismics. Abstract 325, 6th SBGf Mtg., Rio de Janeiro.

Haines, A.J. and de Hoop, M.V., 1996. An invariant embedding analysis of general wave scattering problems. J. Math. Phys., 37: 3854-3881.

Rickett, J.E. and Lumley, D.E., 2001. Cross-equalization data processing for time-lapse seismic reservoir monitoring: A case study from the Gulf of Mexico. Geophysics, 66: 1015-1025.

Wapenaar, C.P.A., Fokkema, J.T., Dillen, M.W.P. and Scherpenhuijsen, P., 2000. One-way acoustic reciprocity and its applications in multiple elimination and time-lapse seismics. Expanded Abstr., 70th Ann. Internat. SEG Mtg., Calgary: 2377-2380.